"Solar-induced fluorescence detects inter-annual variation in gross primary production of coniferous forests in the western United States"

Lauren M. Zuromski[1], David R. Bowling[1,2], Philipp Köhler[3], Christian Frankenberg[3], Michael L. Goulden[4], Peter D. Blanken[5], John C. Lin[1]

[1]Department of Atmospheric Sciences, University of Utah, Salt Lake City, Utah, USA

[2]Department of Biology, University of Utah, Salt Lake City, Utah, USA

[3]California Institute of Technology, Division of Geological and Planetary Sciences, Pasadena, California, USA

[4]Department of Earth System Science, University of California, Irvine, California, USA

[5]Department of Geography, University of Colorado, Boulder, Colorado, USA

Contents of this file

This supporting file provides information on the calculation and utilization of detrended variables, the definitions used for the active GPP_{Tower} seasons, and the spatial degradation of NDVI and EVI.

Detrended data analyses

In order to analyze correlations of SIF, NDVI, EVI, and GPP_{MODIS} with GPP_{Tower}, independent from multi-year trends, these trends were removed from each variable. Detrended data for each variable were determined by fitting a linear regression (with time) over each site's selected record (periods of record shown in Table 1), and then subtracting these trends from the monthly data. Detrended time series of the predictive variables and their linear regressions with GPP_{Tower} (Figure S2) and their standardized annual anomalies (Figure S3) were calculated as with the original data in the main paper (compare Figures 1–2 in the main paper to detrended Figures S2–S3).

The GPP_{Tower} trends at both Niwot and Metolius were not statistically significant ($p > 0.05$, regression not shown), indicating the average annual GPP_{Tower} did not change over their respective periods of record. However, significant decreasing GPP_{Tower} trends occurred at $Sierra_{low}$ ($p < 0.01$, regression not shown) and $Sierra_{high}$ ($p < 0.05$, regression not shown). Generally, at $Sierra_{low}$ and $Sierra_{high}$, detrended NDVI, EVI, and GPP_{MODIS} better predicted seasonal GPP_{Tower} than the original, trended variables, while the GPP_{Tower}-SIF correlations slightly decreased after detrending (compare Figure 1e–h in the main paper with Figure S2e–h). Though detrended NDVI, EVI, and SIF all predicted 39% of seasonal GPP_{Tower} variation at $Sierra_{low}$ (Figure S2e–f), detrended SIF still predicted the most seasonal GPP_{Tower} variation at $Sierra_{high}$ (Figure S2g–h).

When considering inter-annual variation with the detrended data (Figure S3), SIF explained more variation ($r^2 = 0.24$, $p = 0.01$) in GPP_{Tower} than did NDVI ($r^2 = 0.03$, $p = 0.43$), EVI ($r^2 = 0.00$, $p = 0.85$), or GPP_{MODIS} ($r^2 = 0.14$, $p = 0.07$) when all of the sites were grouped together. This is consistent with the results using the original data (Figure 2, main paper). Although linear regressions between GPP_{Tower} and the explanatory variables were generally weak for individual sites (Figure S3), correlations at Niwot were significant for the GPP_{Tower}-SIF ($r^2 = 0.50$, $p = 0.05$), GPP_{Tower}-NDVI ($r^2 = 0.71$, $p = 0.01$), and GPP_{Tower}-GPP_{MODIS} ($r^2 = 0.63$, $p = 0.02$) regressions.

Active GPP_{Tower} season definitions

Since the length of the active GPP_{Tower} season (where GPP_{Tower} is > 0) varied with each site, comparisons were made over three defined time periods 1) a full annual cycle (as described in the main paper), or time periods representing 2) 90% or 3) 70% of the active GPP_{Tower} season (both described here). In each case, inter-annual standardized anomalies of cumulative GPP_{Tower} for the time period were compared to inter-annual standardized anomalies of averaged SIF, NDVI, EVI, or cumulative GPP_{MODIS} using linear regression.

Time period definitions were determined by averaging monthly cumulative GPP_{Tower} over each site's multi-year record to generate an average seasonal cycle for GPP_{Tower}. These average seasonal cycles were then normalized from 0–1 with respect to the individual sites' seasonal minima and maxima (Figure S4a). The normalized seasonal cycles were plotted as cumulative GPP_{Tower} (Figure S4b), and these curves were used to determine the time periods representing the center 90% or 70% of the active GPP_{Tower} season as follows.

The start- and end-months of the growing seasons were chosen based on which months' GPP_{Tower} totals fell closest to 5% and 95% (capturing ~90% of cumulative annual GPP_{Tower}), and 15% and 85% (capturing ~70% of cumulative annual GPP_{Tower}). Specifically, the first months approximating either 5% or 15% of cumulative annual GPP_{Tower} and the last months approximating either 90% or 85% of cumulative annual GPP_{Tower} were selected as bounds for the respective active periods (Table S2). These definitions were chosen to ensure similar proportions of annual GPP_{Tower} were captured between sites, owning to approximate definitions because of the coarse scale of monthly cumulative GPP_{Tower}.

Results of linear regressions of the standardized anomalies (r^2, and statistical significance, if any) are shown in Table S2. When all sites were grouped together, for the 90% active GPP_{Tower} season period, SIF explained 16% of GPP_{Tower} variation ($p < 0.05$), while NDVI ($r^2 = 0.00$, $p > 0.05$), EVI ($r^2 = 0.01$, $p > 0.05$), and GPP_{MODIS} ($r^2 = 0.04$, $p > 0.05$) explain little to none of this variation. However, for the 70% active GPP_{Tower} season, none of the predictor variables explained any GPP_{Tower} variation. Similarly, for individual-site linear regressions, relationships were statistically insignificant, except for regressions at $Sierra_{high}$ for NDVI and EVI for the 90% active GPP_{Tower} season, albeit negatively correlated, and at $Sierra_{low}$ for GPP_{MODIS} for the 70% active GPP_{Tower} season ($r^2 = 0.80$, $p < 0.05$). Although the GPP_{Tower}-SIF relationship that exists when considering whole calendar years was only robust against the 90% active GPP_{Tower} season when all sites were grouped together, the other predictor variables still did not explain any GPP_{Tower} variation for any active season definition.

Spatial degradation for NDVI and EVI

To ensure the fine resolutions of NDVI and EVI (0.05°) did not unnecessarily decrease seasonal and inter-annual correlations with GPP, we also degraded these resolutions to match that of GOME-2 SIF. The area-weighted averages of NDVI and EVI were calculated using each flux tower location as the center point of a 0.5° box surrounding each flux tower site. With these boxes we sought to approximate the average GOME-2 measurement polygon for each location over the years used in the analyses. Within each 0.5° box, we also calculated the percentage each land cover type encompasses of the total vegetated land (Figure S6) using a "present-day", 0.125° surface map dataset compiled by NCAR for simulations with the Community Land Model (v.4.5, available at: https://svn-ccsminputdata.cgd.ucar.edu/trunk/inputdata/lnd/clm2/surfdata_map/surfdata_0.1 25x0.125_simyr2000_c150114.nc).

When utilizing the spatially-coarse NDVI and EVI in the analyses, seasonal correlations with GPP generally increased, while inter-annual correlations remained unchanged (compare Figures 1– 2 in the main paper to Figures S7–S8). Degrading the resolutions of NDVI and EVI showed the greatest improvement for seasonal GPP correlations at $Sierra_{high}$. After spatial degradation, seasonal correlations between NDVI, EVI, and GPP marginally improved, (compare Figure 1 to Figure S7). However, inter-annual variability in GPP was always best correlated with SIF (Figure 2) relative to these other indices.

Figure S1 Locations of the four western U.S. eddy covariance flux towers used in this study, superimposed on a map of the western U.S. Boundaries between states are visible. Site details can be found in Table 1.
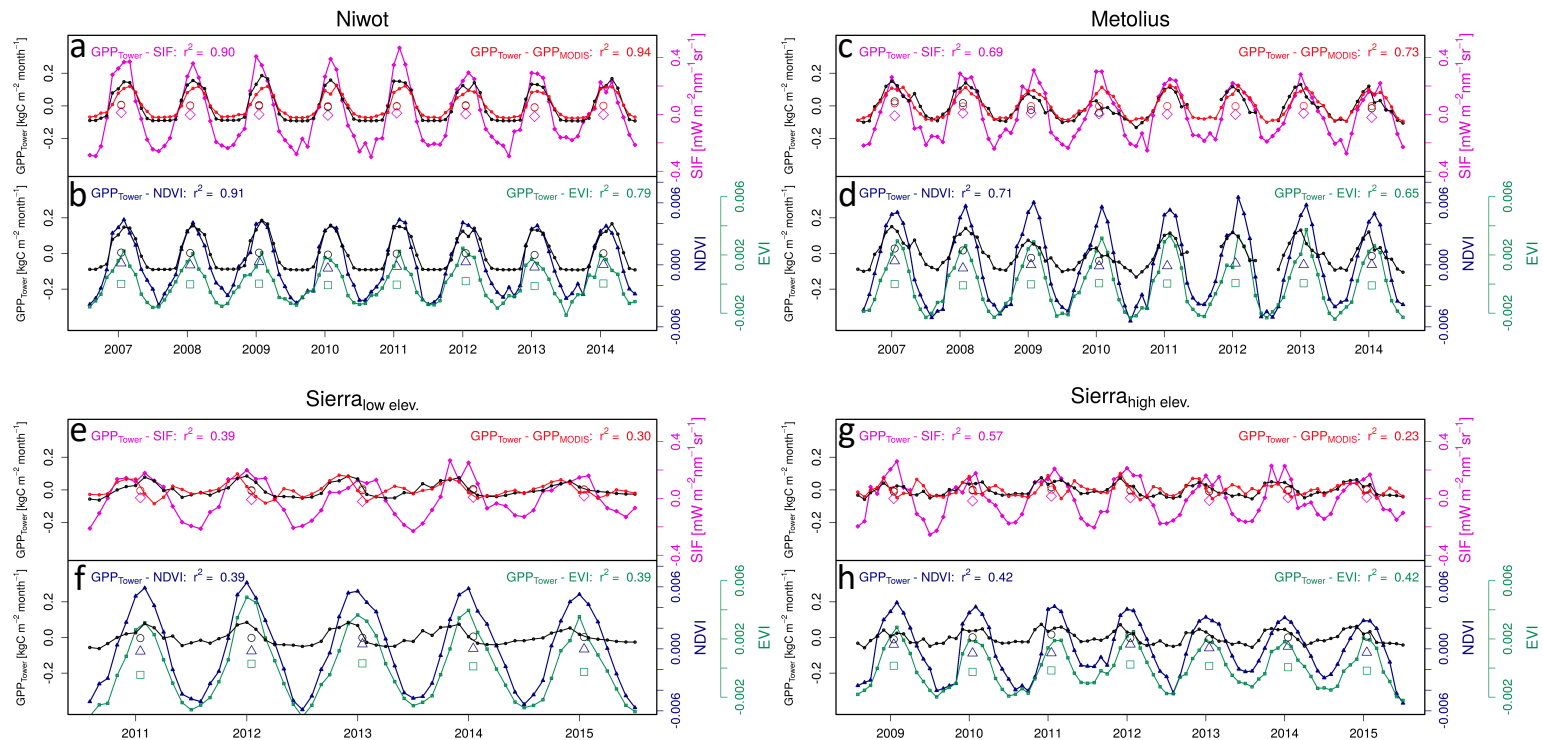
Figure S2 As in Figure 1, main paper, but the time series have been linearly detrended. Multi-year time series of monthly cumulative GPP_{Tower} from observations at four flux towers (black, circle), SIF (purple, diamond), NDVI (blue, triangle), EVI (green, square), and GPP_{MODIS} (red, circle) are shown. NDVI and EVI were weighted by solar radiation. The annual average value for each variable is shown as a larger symbol (of each variable's respective color and shape), plotted at June of each year. The r^2 values correspond to the linear regressions between GPP_{Tower} and SIF (purple), GPP_{Tower} and NDVI (blue), GPP_{Tower} and EVI (green), and GPP_{Tower} and GPP_{MODIS} (red) on a monthly basis.
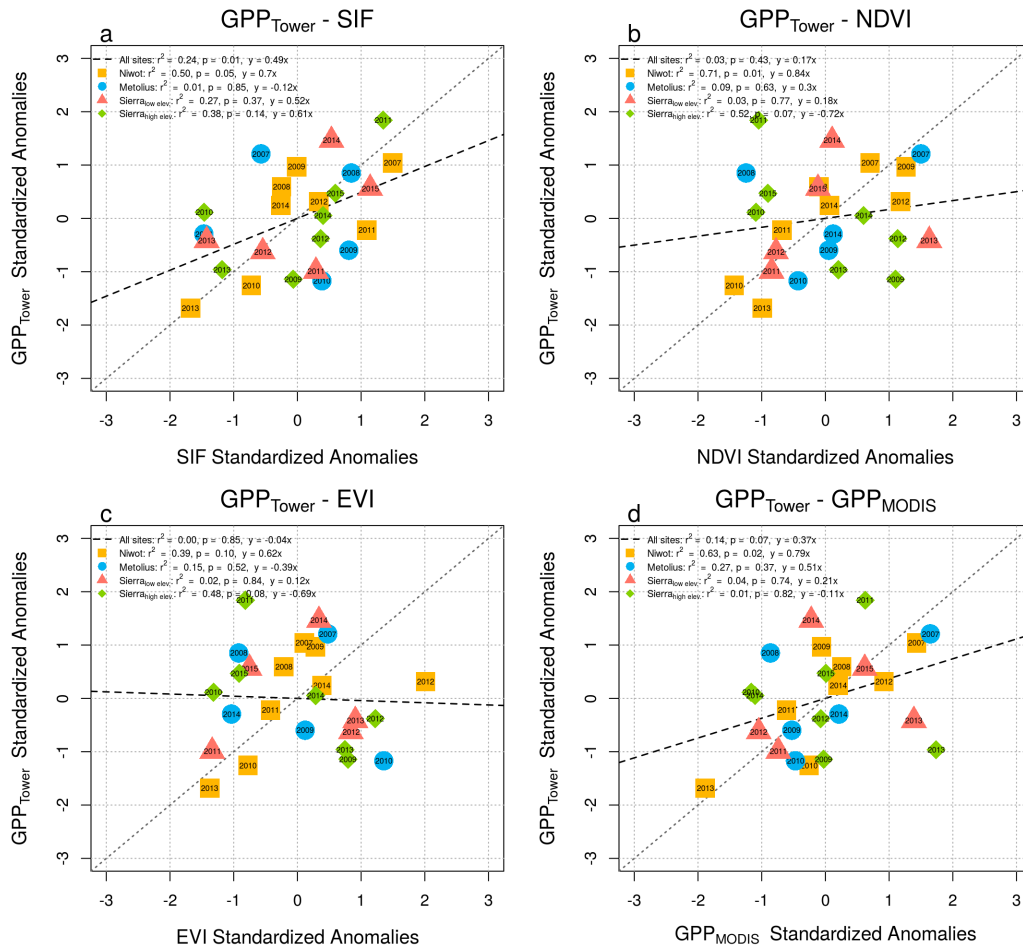
Figure S3 As in Figure 2, main paper, but using detrended variables. Scatter plots of GPP$_{Tower}$ annual standardized anomalies compared to those for SIF (a), NDVI (weighted by solar radiation) (b), EVI (weighted by solar radiation) (c), and GPP$_{MODIS}$ (d). The symbols are coded in both color and shape, with years indicated on the symbol. Site-level r^2 values and p-values are indicated next to the site name. The multi-site r^2 and p-values are also specified, with a corresponding linear regression, indicated by a dashed line. A 1:1 dotted line is shown for reference.
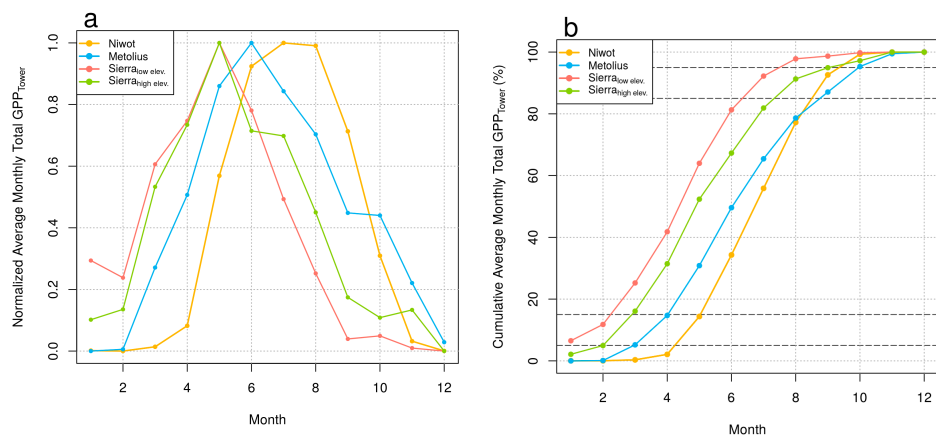
Figure S4 (a) Normalized average monthly cumulative GPP_Tower for each site, illustrating the difference in timing of the GPP active season. (b) Cumulative monthly GPP_Tower from (a), converted into percentages of cumulative GPP_Tower. Horizontal lines in order from the bottom to the top, respectively, indicate: 5%, 15%, 85%, and 90% of the annual total GPP_Tower.
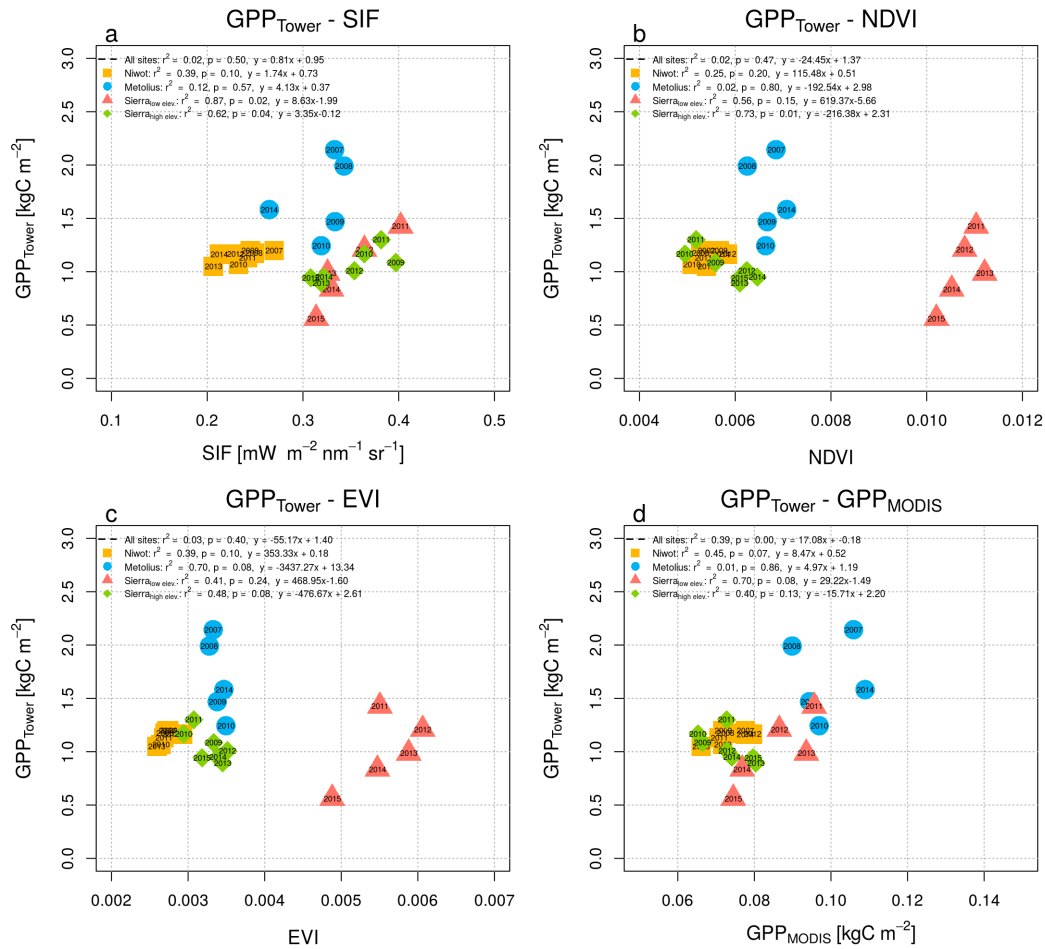
Figure S5 Scatter plots of cumulative annual GPP_Tower plotted versus SIF (a), NDVI (weighted by solar radiation) (b), and EVI (weighted by solar radiation) (c) annual averages, and cumulative annual GPP_MODIS (d). These contrast with Figure 2 in that they have not been converted to standardized anomalies, but they were calculated from the original time series (Figure 1) and not the detrended time series (Figure S2). The symbols are coded in both color and shape, with years indicated on the symbol. Site-level r^2 values and p-values are indicated next to the site name. The multi-site r^2 and p-values are also specified, with a corresponding linear regression, indicated by a dashed line. A 1:1 dotted line is shown for reference in the GPP_Tower-GPP_MODIS scatter plot.
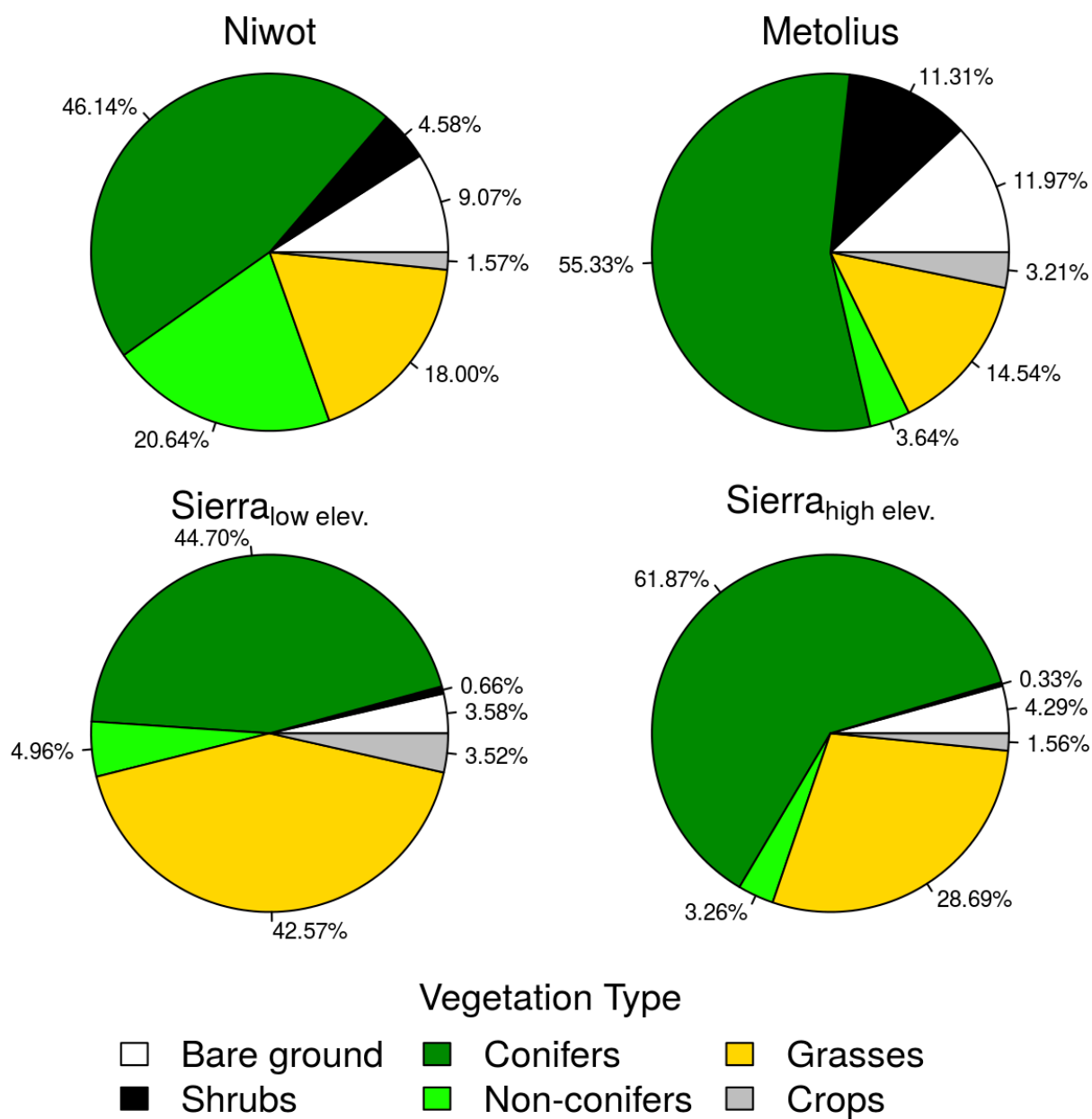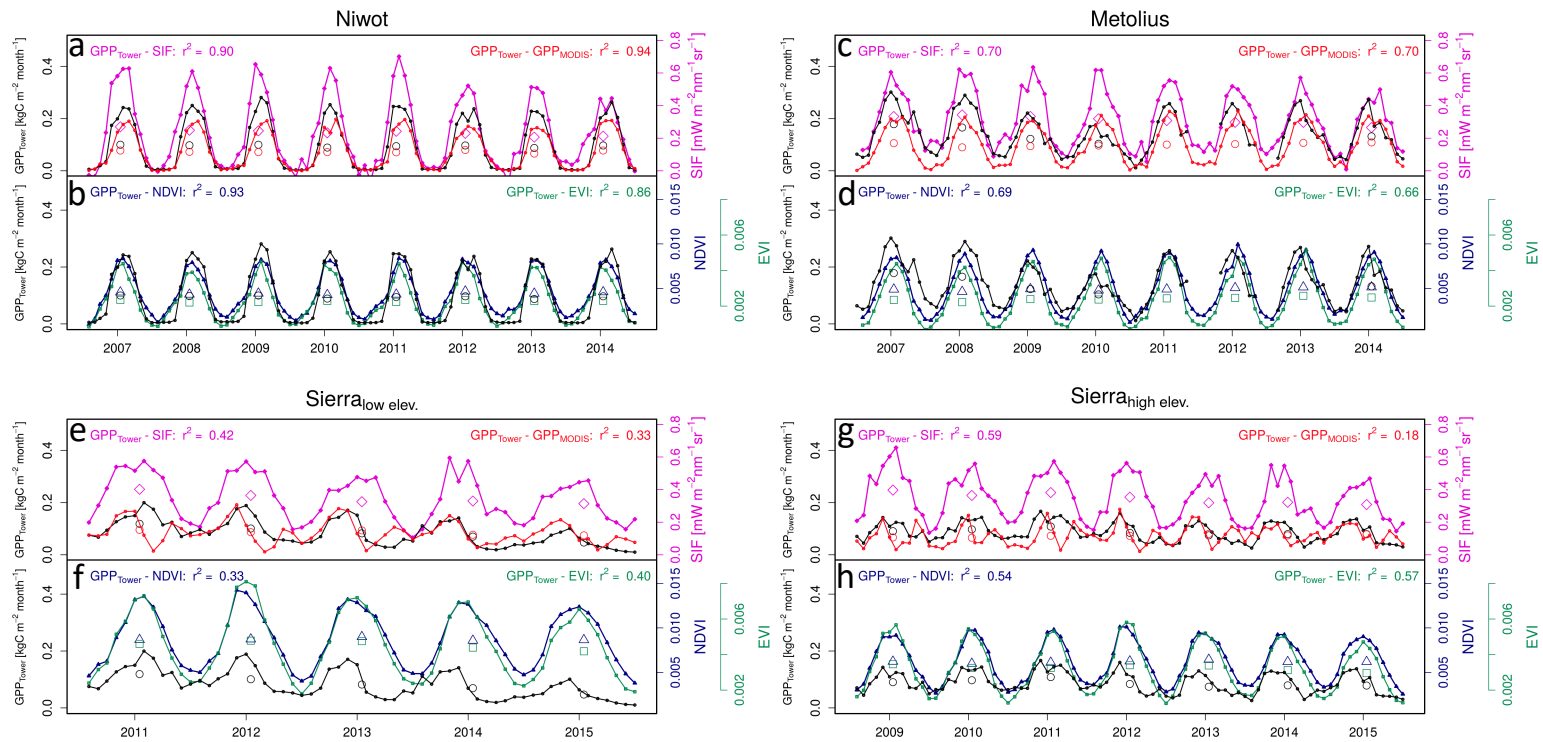
Figure S6 Percentages of land cover types within a 0.5° box encompassing each flux tower site. For simplicity, groups were classified broadly as: bare ground (no vegetation), shrubs, conifers, non-conifers (broadleaf evergreen and deciduous trees, and broadleaf evergreen trees), grasses, and crops.

Figure S7 As in Figure 1, main paper, but using spatially-degraded NDVI and EVI. Multi-year time series of monthly cumulative GPP_{Tower} from observations at four flux towers (black, circle), SIF (purple, diamond), NDVI (blue, triangle), EVI (green, square), and GPP_{MODIS} (red, circle) are shown. NDVI and EVI were weighted by solar radiation. The annual average value for each variable is shown as a larger symbol (of each variable's respective color and shape), plotted at June of each year. The r^2 values correspond to the linear regressions between GPP_{Tower} and SIF (purple), GPP_{Tower} and NDVI (blue), GPP_{Tower} and EVI (green), and GPP_{Tower} and GPP_{MODIS} (red) on a monthly basis.
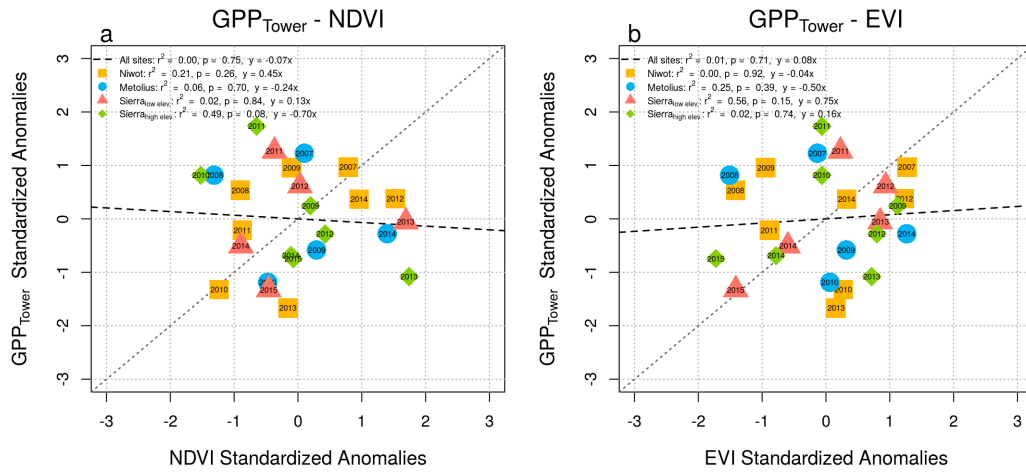
Figure S8 As in Figure 2, main paper, but using spatially-degraded NDVI and EVI. Scatter plots of GPP_{Tower} annual standardized anomalies compared to those for NDVI (weighted by solar radiation) (a) and EVI (weighted by solar radiation) (b). The symbols are coded in both color and shape, with years indicated on the symbol. Site-level r^2 values and p-values are indicated next to the site name. The multi-site r^2 and p-values are also specified, with a corresponding linear regression, indicated by a dashed line. A 1:1 dotted line is shown for reference.

Site name	Monthly CV	Yearly CV
Niwot	1.02	0.05
Metolius	0.76	0.26
Sierra$_{low\ elev.}$	0.76	0.30
Sierra$_{high\ elev.}$	0.72	0.28

Table S1 Coefficients of variation (CV, dimensionless) for GPP_{Tower} at each site, based on monthly time series or on cumulative annual GPP_{Tower} (as in Figure 1).

Site name	Cumulative annual GPP$_{Tower}$				~90% cumulative annual GPP$_{Tower}$					~70% cumulative annual GPP$_{Tower}$				
	SIF	NDVI	EVI	GPP$_{MODIS}$	SIF	NDVI	EVI	GPP$_{MODIS}$	Active season	SIF	NDVI	EVI	GPP$_{MODIS}$	Active season
Niwot	0.39	0.25	0.39	0.45	0.14	0.36	0.22	0.32	Apr–Sept	0.23	0.00	0.03	0.03	May–Aug
Metolius	0.12	0.02	0.70	0.01	0.05	0.02	0.20	0.03	Mar–Sept	0.01	0.00	0.14	0.13	Apr–Aug
Sierra$_{low\ elev.}$	0.87*	0.56	0.41	0.70	0.37	0.16	0.34	0.70	Jan–Jul	0.07	0.17	0.37	0.80*	Feb–Jun
Sierra$_{high\ elev.}$	0.62*	0.73*	0.48	0.40	0.23	0.67*	0.78*	0.43	Feb–Aug	0.12	0.02	0.00	0.00	Mar–Jun
All sites	0.46 ****	0.00	0.00	0.05	0.16*	0.00	0.01	0.04	--	0.02	0.01	0.00	0.10	--

Table S2 Coefficients of determination (r^2) for linear regressions between standardized anomalies of GPP$_{Tower}$ and SIF, NDVI, EVI, or GPP$_{MODIS}$. These are shown separately for the three different GPP$_{Tower}$ active season definitions. Statistical significance is indicated: * = $p < 0.05$, ** = $p < 0.01$, *** = $p < 0.001$, **** = $p < 0.0001$.

Site name		Seasonally				Annually			
		r^2	p-value	Regression	n	r^2	p-value	Regression	n
Niwot	SIF	0.90****	0.00	y = 0.42x	96	0.39	0.10	y = 1.74x + 0.73	8
	NDVI	0.90****	0.00	y = 34.12x − 0.09	96	0.25	0.20	y = 115.48x + 0.51	8
	EVI	0.79****	0.00	y = 72.04x − 0.10	96	0.39	0.10	y = 353.33x + 0.18	8
	GPP$_{MODIS}$	0.94****	0.00	y = 1.34x	96	0.45	0.07	y = 8.47x + 0.52	8
Metolius	SIF	0.70****	0.00	y = 0.37x + 0.02	89	0.12	0.57	y = 4.13x + 0.37	5
	NDVI	0.69****	0.00	y = 17.31x + 0.02	89	0.02	0.80	y = -192.54x + 2.98	5
	EVI	0.63****	0.00	y = 32.73x + 0.03	89	0.70	0.08	y = -3437.27x + 13.34	5
	GPP$_{MODIS}$	0.70****	0.00	y = 0.88x + 0.05	89	0.01	0.86	y = 4.97x + 1.19	5
Sierra$_{low\ elev.}$	SIF	0.42****	0.00	y = 0.24x	60	0.87*	0.02	y = 8.63x − 1.99	5
	NDVI	0.32****	0.00	y = 7.25x + 0.01	60	0.56	0.15	y = 619.37x − 5.66	5
	EVI	0.34****	0.00	y = 12.30x + 0.02	60	0.41	0.24	y = 468.95x − 1.60	5
	GPP$_{MODIS}$	0.33****	0.00	y = 0.66x + 0.03	60	0.70	0.08	y = 29.22x − 1.49	5
Sierra$_{high\ elev.}$	SIF	0.59****	0.00	y = 0.20x + 0.02	84	0.62*	0.04	y = 3.35x − 0.12	7
	NDVI	0.34****	0.00	y = 7.91x + 0.04	84	0.73*	0.01	y = -216.38x + 2.31	7
	EVI	0.38****	0.00	y = 16.51x + 0.03	84	0.48	0.08	y = -476.67x + 2.61	7
	GPP$_{MODIS}$	0.18****	0.00	y = 0.43x + 0.06	84	0.40	0.13	y = -15.71x + 2.20	7

Table S3 Results of linear regression of GPP$_{Tower}$ and SIF, NDVI, EVI, or GPP$_{MODIS}$, based on monthly time series (as in Figure 1), or on cumulative annual GPP$_{Tower}$ (Figure S5). Statistical significance is indicated: * = $p < 0.05$, ** = $p < 0.01$, *** = $p < 0.001$, **** = $p < 0.0001$.